Raptor Coding of H.264/AVC Data-Partitioned Video over a WiMAX Channel

Laith Al-Jobouri, Martin Fleury, *Member*, IEEE, and Mohammed Ghanbari, *Fellow*, IEEE

Abstract — *This paper demonstrates robust video streaming for IPTV over an IEEE 802.16e (WiMAX). In the proposed method, an H.264/AVC video bit-stream is data partitioned according to source coding priority. Raptor channel coding is adaptively applied to the partitioned data. In the event of outright packet drops, redundant partition bearing packets serve to protect priority data. Further, to guarantee a minimum acceptable level of video quality, additional intra-refresh macro-blocks reduce the effect of temporal error propagation[1].*

Index Terms — WiMAX, video streaming, Raptor channel coding, IPTV

I. INTRODUCTION

This paper's contribution is ways of improving the robustness of data-partitioned streaming in the context of IPTV over a broadband wireless channel. A key issue for data-partitioned streaming [1] is how to provide protection against a harsh channel environment. In an H.264/AVC (Advanced Video Coding) codec [2], when data-partitioning is enabled, every slice is divided into three separate partitions: partition-A (has the most important data, motion vectors); -B (intra coefficients); and -C (inter coefficients, with the least important data). These data are packed into three types of Network Abstraction Layer units (NALU's). The importance of each NALU-bearing packet is identified in the NALU header. This paper considers outright packet drops through burst errors due to a mobile device entering a deep fade, caused by a change of wireless environment. The paper also caters for packets that are corrupted but may still be repairable by Raptor channel coding [3]. In the latter case, the error bursts occur at the byte-level, resulting in corrupted packets, as may arise from fast fading due to multipath reception over an IEEE 802.16e (mobile WiMAX) channel [4].

For further improvement to the robustness, intra-refresh (IR) macro-blocks (MB's) are employed rather than periodically refreshing the whole picture. The IR MB's are either randomly placed up to a given percentage within any one picture or are included as one line of MB's per picture in a cyclic configuration. This provision avoids the high data-rate spikes of periodic, intra-coded I-pictures, which can disrupt bandwidth-limited wireless communication.

[1] L. Al-Jobouri, M. Fleury and M. Ghanbari are with the University of Essex, Colchester, CO4 3SQ UK (e-mail: {lamoha, fleum, ghan@essex.ac.uk).

Data-partitioning [5] involves the rearrangement of the compressed bitstream at the slice level, according to the reconstruction priority of the data components. There is less overhead than other forms of resilience such as Flexible Macroblock Ordering [1] and, hence, data-partitioning can operate during favorable channel conditions, as well as unfavorable channel conditions. Our scheme allows graceful degradation in the face of channel error, and in worsening channel conditions, duplicate packets are transmitted. This is because, though application-layer (AL) forward error correction (FEC) can protect against packet corruption, when the overhead from FEC is large or when packets are likely to be corrupted or dropped before reaching the application, it is then preferable to transmit duplicates. On the other hand, the duplicate slice stream should be turned off during favorable channel conditions, as its transmission involves a significant overhead. It is possible to send redundant pictures slices [6], which employ a coarser quantization than the main stream, but this can lead to encoder-decoder drift. Besides, replacing one partition with a redundant slice with a different quantization parameter (QP) to the other partitions would not permit reconstruction in an H.264/AVC codec.

To achieve adaptation (and also to turn off duplicate slices during favorable conditions) channel estimation is necessary. As an example, the IEEE 802.16e standard [4] specifies that a station should provide channel measurements, which can either be Received Signal Strength Indicators or may be Carrier-to-Noise-and-Interference Ratio measurements made over modulated carrier preambles. Therefore, to aid in this process the proposed method assumes one of these methods is implemented.

Rateless channel coding is applied at the application layer as an erasure correction code. AL-FEC has been found necessary [7] for a number of error-prone network environments, because of the stringent anticipated requirements for IPTV. The Digital Video Broadcast project has specified [8] optional application-layer rateless coding, though not adaptive as herein. Similarly, 3GPP have also specified a rateless scheme [9], though again not an adaptive coding one.

IPTV is anticipated to be a key application of broadband wireless access networks such as mobile WiMAX, now being deployed in rural areas and in developing countries with a limited 3G infrastructure. However, 'bursty' errors can still disrupt a fragile compressed video bitstream, because of the source coding dependencies, which arise both from motion-

compensated prediction and entropy coding within the codec. Consequently, those videos with high source coding complexity are at risk, because of larger packet sizes and because of the difficulty of reconstructing pictures through error concealment, when prior or neighboring data are missing.

The remainder of this paper is organized as follows. Section II introduces essential background to understanding of the paper. Section III outlines the protection method used and describes the simulation model employed. Section IV evaluates the protection scheme in respect to the use of duplicated data. Finally, Section V concludes the paper.

II. BACKGROUND

In this Section, rateless channel coding and data-partitioning are principally introduced. Some results are also given to explain the interest in data-partitioning.

A. Rateless Codes

Rateless or Fountain coding [10], of which Raptor coding [3] is a subset, is ideally suited to a binary erasure channel in which either the error-correcting code works or the channel decoder fails and reports that it has failed. In erasure coding, all is not lost as flawed data symbols may be reconstructed from a set of successfully received symbols (if sufficient of these symbols are successfully received). A fixed-rate (n, k) Reed-Solomon (RS) erasure code over an alphabet of size $q = 2^L$ has the property that if *any* k out of the n symbols transmitted are received successfully then the original k symbols can be decoded. However, in practice not only must n, k, and q be small but also the computational complexity of the decoder is of order $n(n - k) \log_2 n$. The erasure rate must also be estimated in advance.

The class of Fountain codes [10] allows a continual stream of additional symbols to be generated in the event that the original symbols could not be decoded. It is the ability to easily generate new symbols that makes Fountain codes rateless. Decoding will succeed with small probability of failure if any of k $(1 + \varepsilon)$ symbols are successfully received. In its simplest form, the symbols are combined in an exclusive OR (XOR) operation, according to the order specified by a random, low density generator matrix and, in this case, the probability of decoder failure is $\partial = 2^{-k\varepsilon}$, which, for large k, approaches the Shannon limit. The random sequence must be known to the receiver but this is easily achieved, through knowledge of the sequence seed.

Luby transform (LT) codes [11] reduce the complexity of decoding a simple Fountain code (which is of order k^3) by means of an iterative decoding procedure. The 'belief propagation' decoding relies on the column entries of the generator matrix being selected from a robust Soliton distribution. In the LT generator matrix case, the expected number of degree one combinations (no XORing of symbols) is $S = c \ln(k/\partial)\sqrt{k}$, for small constant c. Setting $\varepsilon = 2 \ln(S/\partial)\, S$ ensures that, by sending $k(1 + \varepsilon)$ symbols, these symbols are decoded with probability $(1 - \partial)$ and decoding complexity of order $k \ln k$.

Encoding of the LT, in the form used in this paper, is accomplished as follows: Choose d_i randomly from some distribution of degrees, where $\rho_{di} = Pr[\text{degree } d_i]$, Pr is the probability of a given event. Choose d_i random information symbols R_i among the k information symbols. These R_i symbols are then *XOR*ed together to produce a new composite symbol, which forms one symbol of the transmitted packet. Thus, if the symbols are bytes then all of the R_i byte's bits are *XOR*ed with all of the bits of the other randomly selected bytes in turn. It is not necessary to specify the random degree or the random symbols chosen if it is assumed that the (pseudo-) random number generators of sender and receiver are synchronized, as mentioned above.

Symbols are processed at the decoder as follows. If a symbol arrives with degree greater than one, it is buffered. If a clean symbol arrives with degree one then it is *XOR*ed with all symbols in which it was used in the encoding process. This reduces the degree of each of the symbols to which the degree one symbol is applied. When a degree two symbol is eventually reduced to degree one, it too can be used in the decoding process. Notice that a degree one symbol is a symbol for which no *XOR*ing has taken place. Notice also that for packet erasure channels a clean degree one symbol (a packet) is easily established as such.

The degree distribution used in [11] (the ideal Soliton distribution) is given by:

$$\rho(1) = 1/n \tag{1}$$

$$\rho(d) = \frac{1}{d(d-1)}, \qquad d = \{2, 3, \ldots, k\} \tag{2}$$

where k is the number of source symbols. In practice, the robust Soliton distribution [10] is employed, as this produces degree-one symbols at a more convenient rate for decoding. It also avoids isolated symbols that are not used elsewhere. Two tuneable parameters [10], c and δ, are used to form the expected number of useable degree one symbols:

$$S = c \ln\left(\frac{k}{\delta}\right)\sqrt{k} \tag{3}$$

where c is a constant close to 1 and δ is a bound on the probability that decoding fails to complete. Then define

$$\begin{aligned} \tau(d) &= \frac{S}{k}\frac{1}{d} && \text{for } d = 1, 2, \ldots (k/S)\text{-}1 \\ &= \frac{S}{k}\ln\left(\frac{S}{\delta}\right) && \text{for } d = k/S \\ &= 0 && \text{for } d > k/S \end{aligned} \tag{4}$$

as an auxiliary positive-valued function to give the robust Soliton distribution:

$$\mu(d) = \frac{\rho(d) + \tau(d)}{z} \tag{5}$$

where z normalizes the probability distribution to unity and is given by:

$$z = \sum_d (\rho(d) + \tau(d)) \quad . \tag{6}$$

The essential differences between Fountain erasure codes and RS erasure codes are that: Fountain codes in general (not Raptor codes [3]) are not systematic; and that, even if there were no channel errors, there is a small probability that the decoding will fail. In compensation, they are completely flexible, have linear decode computational complexity, and generally their overhead is considerably reduced compared to fixed erasure codes. Apart from the startling reduction in computational complexity, a Raptor code has the maximum distance separable property. That is, the source packets can be reconstructed with high probability from any set of *k* or just slightly more than *k* received symbols. A further advantage of Raptor coding is that it does not share the high error floors on a binary erasure channel [12] of prior rateless codes.

B. Data partitioning

In an H.264/AVC codec, the Network Abstraction Layer facilitates the delivery of the Video Coding Layer data to the underlying transportation protocols such as RTP/IP, H.32X and MPEG-2 systems. Each NALU can be considered as a packet that contains an integer number of bytes including a header and a payload. The header specifies the NALU type and the payload contains the related data. When data partitioning is enabled, every slice is divided into three separate partitions and each partition is located in either of type 2 to type-4 NALU's, as listed in Table I. A NALU of type 2, also known as partition-A, comprises the most important information of the compressed video bit stream of P- and B-pictures, that is the MB addresses, motion vectors (MV's) and essential headers. If any MB's in these pictures are intra-coded, their integer-valued Discrete Cosine Transform (DCT) coefficients are packed into the type-3 NALU, also known as partition-B. Type 4 NAL, also known as partition-C, carries the DCT coefficients of the motion-compensated inter-picture coded MB's. Partitions A and B of data-partitioned P- and B-slices are small for broadcast quality video but their C-type partitions can be very long.

Data partitioning is a form of source-coded error resilience [1]. Combining, error resilience with error control involves additional data overhead. However, Fig. 1 shows that, of four common error resilience tools in H.264/AVC, data partitioning has the least overhead. The illustration is the well-known *Foreman* clip representing the jerky motion of a hand-held camera with a rapid pan towards the end of the sequence. In Fig. 1, the horizontal axis represents the mean bitstream rate arrived at by setting the QP to the given value, while the vertical axis represents the mean overhead rate with that QP. As the quality decreases (higher QP), the advantage of data-partitioning increases, as the relative overhead of all schemes increases. Tests of the *Akiyo*, *Coastguard*, and *Mobile* sequences, show that the overhead is not strongly dependent on coding complexity, with the size of overhead ordering between the schemes preserved.

The relative mean sizes (across all frames in the sequence) of the data partitions for a sequence with higher spatial coding complexity, *Paris*, and one with high temporal coding complexity, *Stefan*, were examined. The results for these sequences are reported in Table II according to video quality

TABLE I. NALU TYPES

NAL unit type	Class	Content of NAL unit
0	-	Unspecified
1	VCL	Coded slice
2	VCL	Coded slice partition-A
3	VCL	Coded slice partition-B
4	VCL	Coded slice partition-C
5	VCL	Coded slice of an IDR picture
6-12	Non-VCL	Suppl. info., parameter sets, etc.
13-23	-	Reserved
24-31	-	Unspecified

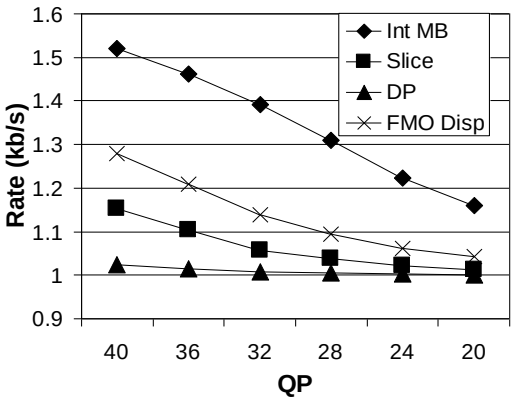

Fig. 1. QCIF *Foreman* rates according to QP (horizontal axis) plotted against overhead rate (vertical axis) arising from H.264 error resilience tool: Int MB = Intra-coded macroblock refresh, FMO Disp = Flexible Macroblock Ordering dispersed mode (two slices), DP = data-partitioning, Slice = slice structuring with 3 slices per frame.

TABLE II. RELATIVE SIZES OF PARTITIONS A, B, AND C FOR VIDEO SEQUENCES *PARIS* AND *STEFAN* ACCORDING TO VIDEO QUALITY

QP	*Paris*			*Stefan*		
	A	B	C	A	B	C
20	11%	9%	80%	5%	5%	90%
30	33%	11%	56%	36%	9%	55%
40	66%	12%	22%	62%	10%	28%

(PSNR) given by the QP setting. Both sequences were encoded at Common Intermediate Format (CIF) (352×288 pixel/frame), with a Group of Picture (GoP) structure of IPPP….. at 30 Hz (frame/s). Experiments not shown indicate that including B-pictures, with a GoP structure of IPBP (sending order) … and intra-refresh rate of 15, did not noticeably disturb this pattern.

C. Intra-refresh macroblocks

The insertion of IR MBs into pictures [13] normally encoded through motion-compensated prediction allows temporal error propagation to be arrested if matching MB's in a previous picture are lost. In the H.264/AVC JM implementation, various IR schemes exist such as random, which sets a maximum percentage of intra-coded MB's, or cyclic, which replaces each line of the picture in turn in cyclic order. Notice that naturally encoded intra-coded MBs are also inserted into predictively-coded P-pictures when inter-coding brings limited or no advantage. For example, this may occur during rapid motion or when a new object that is not present in a previous

TABLE III. TOTAL NALU SIZES IN BYTES FOR DIFFERENT IR MB PERCENTAGES AND MB LINE INTRA UPDATE FOR CIF PICTURES IN THE *FOOTBALL* SEQUENCE

QP	2% Intra-refresh MB			5% Intra-refresh MB		
	A	B	C	A	B	C
20	1842	2678	3889	1845	2767	3867
25	1687	1697	2533	1690	1763	2511
30	1459	1047	1496	1463	1082	1482
35	1117	572	688	1120	595	682
QP	25% Intra-refresh MB			MB Line Intra Update		
	A	B	C	A	B	C
20	1893	3450	3669	1885	3385	3683
25	1746	2216	2379	3683	2160	2400
30	1505	1346	1405	1498	1312	1414
35	1146	729	646	1143	716	652

picture is uncovered. The inclusion of IR MBs does lead to some increase in the size of partition-B bearing packets, as shown in Table III for different QPs and percentages of IR MBs. The sequence is *Football* with high temporal coding complexity, encoded with the same configuration as in Section II.B. It is also possible to vary the IR rate according to scene type or channel conditions [14].

III. METHODOLOGY

Three types of erroneous packets were considered: 1) packet drops at a WiMAX base station (BS) sender buffer 2) packet drops through channel noise and interference, and 3) corrupted packets that were received but affected by channel noise, to the extent that they could not be immediately reconstructed without an Automatic Repeat reQuest (ARQ) triggered retransmission of additional redundant data. Additional redundant data were piggybacked onto the next packet. Notice that if the retransmission of additional redundant data still fails to allow the original packet to be reconstructed then the packet was simply dropped. This allows video-rate transmission to be maintained, especially as the single ARQ is returned within the WiMAX return sub-frame. In this paper, as sub-packet symbols, namely bytes, are used, then a Cyclic Redundancy Check (CRC) retrospectively determines whether all bytes in a packet have been reconstructed. It is assumed that data are checked for successful receipt at the wireless PHYsical layer, and only successfully received data are passed up through the layers of the protocol stack.

Raptor channel coding was applied to decide if a packet could be recovered, given the number of bytes that were declared to be in error. As Raptor channel coding is linear in complexity at the encoder and decoder, again real-time operation is preserved. Different redundant NALU schemes were trialled to replace dropped packets (erroneous packets of type 1 and 2) as an additional type of protection. Either duplicate partition-A NALU bearing packets were sent, or duplicate partition-A and -B packets, or all three partitions were sent, resulting in a duplicate stream.

In order to model Raptor coding, the following statistical model [15] was employed:

$$P_f(m,k) = 1 \quad \text{if } m < k,$$

$$= 0.85 \times 0.567^{m-k} \text{ if } m \geq k, \qquad (7)$$

where $P_f(m,k)$ is the failure probability of the code with k source symbols if m symbols have been received.

A. WiMAX configuration

The PHY layer settings selected for WiMAX simulation are given in Table IV. The antenna heights and transmit power levels are typical ones taken from the Standard [4]. The antenna is modeled for comparison purposes as a half-wavelength dipole, whereas a sectored set of antenna on a mast might be used in practice to achieve directivity and, hence, better performance. Similarly, multiple-input multiple-output (MIMO) antennas are not modeled. The IEEE 802.16e Time Division Duplex (TDD) frame length was set to 5 ms, as only this value is supported [16] in the WiMAX forum adaptation of the Standard. The data rate results from the use of one of the mandatory coding modes [4] for a TDD downlink/uplink sub-frame ratio of 3:1. The BS was assigned more bandwidth capacity than the uplink from the mobile station (MS) to allow the WiMAX BS to respond if necessary to multiple mobile devices.

Thus, the parameter settings in Table IV such as the modulation type and PHY coding rate are required to achieve a datarate of 10.67 Mbps over the downlink. Buffer sizes were set to 50 packets (a single Medium Access Control (MAC) Service Data Unit within a MAC Protocol Data Unit). This buffer size was selected as appropriate to mobile, real-time applications for which larger buffer sizes might lead both to increased delay and larger memory energy consumption in mobile devices. As a point of comparison, capacity studies [16] suggest up to 16 mobile TV users per mobile WiMAX cell in a 'lossy' channel depending on factors such as the form of scheduling and whether MIMO is activated.

B. Channel configuration

We introduced a two-state Gilbert-Elliott channel model [17] in the physical layer of the simulation to simulate the channel model for WiMAX. To model the effect of slow fading at the packet-level, the P_{GG} (probability of being in a good state) was set to 0.95, P_{BB} (probability of being in a bad state) = 0.96, P_G (probability of packet loss in a good state) = 0.02 and P_B (probability of packet loss in a bad state) = 0.01 for the Gilbert-Elliott parameters. The two hidden states were modeled with Uniform distributions with the stated mean probabilities of packet loss.

Additionally, it is still possible for a packet not to be dropped in the channel but, nonetheless, to be corrupted through the effect of fast fading (or other sources of noise and interference). This byte-level corruption was modeled by a second Gilbert-Elliott model, with the same parameters (applied at the byte level) as that of the packet-level model except that P_B (probability of byte loss) was increased to 0.165 The main intention of the use of this twofold Gilbert-Elliott model was to show the response of the protection scheme to both types of fading (slow as well as fast). The Gilbert-Elliott scheme though simple has been widely adopted, as it is thought to realistically model the burst errors that do occur and, more significantly, can be particularly damaging

TABLE IV. WiMAX SIMULATION PARAMETERS.

Parameter	*Value*
PHY, Duplexing mode	OFDMA, TDD
Frequency, Modulation	5 GHz, 16-QAM 1/2
Frame length	5 ms
Max. packet length	1024 B
Raw data-rate	10.67 Mbps
FFT size, Guard band ratio	1024, 1/8
DL/UL ratio	3:1
Fragmentation	Yes
MS/BS transmit power	250 mW, 20 W
Range	0.7 km
MS/BS antenna heights	1.5/32 m
Antenna type, gain	Omni-directional, 0 dBD

OFDMA=Orthogonal Frequency Division Multiple Access, QAM = Quadrature Amplitude Modulation

to compressed video streams, because of the predictive nature of source coding. Therefore, the impact of 'bursty' errors [18] should be assessed in video streaming applications.

C. Video configuration

The tests were performed on the reference *Football* video sequence (see Section II.C) encoded in CIF @ 30 Hz. The video stream was transmitted to a MS and, to introduce sources of traffic congestion, a permanently available FTP source was introduced with TCP transport to a second MS. Likewise, a Constant Bit-Rate (CBR) source with packet size of 1000 B and inter-packet gap of 0.03s was also downloaded to a third MS.

IV. EVALUATION

Football was encoded using the H.264/AVC reference software JM 14.2 and trace files with different QP's were input into the well-known ns-2 simulator to model transmission across a WiMAX channel. A module from the Change Gung University, Taiwan [19] proved an effective way of modeling IEEE 802.16e's behavior.

Figs. 2–6 presents the results with and without duplicate NALU's with 5% intra refresh MBs. From Fig. 2, the larger packet drop rates at QP = 20 will have a significant effect on the video quality, especially when partition-B and partition-C duplicate NALU's are sent. However, the percentage of dropped packets (through buffer overflow and channel drops from simulated slow fading), reduces considerably for higher QP's (and smaller NALU's). Notice that a percentage for a duplicate NALU scheme is a percentage of all packets sent, whether a packet is classed as duplicate or not.

Fig. 3 shows the pattern of corrupted packet losses arising from simulated fast fading. The effect of the corrupted packets on video quality only occurs if a packet cannot be reconstructed, after application of the AL-FEC scheme with Raptor channel coding and after the adaptive retransmission scheme has been applied. Therefore, though the percentages of corrupted packets are high in Fig. 3, most packets are repairable but only after a delay from the single retransmission of additional redundant data permitted. The effect of QP in reducing packet size is a slow decline in the number of packets corrupted but the decline is not enough to be significant. The percentage of corrupted packets for the duplicate NALU schemes with additional partition-B and partition-C NALU's only occurs at QP's for which the outright packet losses are high. Therefore, the gain for using duplicate NALU's is negated.

Examining Fig. 4 for the resulting objective video quality, one sees that data partitioning with AL-FEC protection, when used without duplication, is insufficient to bring the video quality to above 31 dB, that is to a 'good' quality. PSNRs above 25 dB, we rate as of 'fair' quality (depending on content and coding complexity). However, it is important to note that sending duplicate partition-A packets alone (without duplicate packets from other partitions) is also insufficient to raise the video quality to a 'good' quality (above 31 dB). Therefore, to raise the video quality to a good level (above 31 dB) requires not only the application of the adaptive rateless channel coding scheme but also the sending of duplicate data streams.

Figs. 5 and 6 examine end-to-end delay which is largely determined by packet size and whether a packet has been retransmitted. The impact of corrupted packets, given the inclusion of retransmitted extra redundant data, is largely seen in additional delay. There is an approximate doubling in per-packet delay between the total end-to-end delay for corrupted packets and normal packet end-to-end delay. Normal packets do not, of course, experience the additional delay of a further retransmission prior to reconstruction at the decoder. Therefore, the main penalty arising under the FEC protection scheme from an increased percentage of corrupted packets is an overall increase in delay. Nevertheless, the delays remain in the tens of millisecond range, except for when QP = 20, when end-to-end delay for the scheme with a complete duplicate stream exceptionally is as high as 130 ms. Notice though that for the duplicate stream schemes there is up to twice the number of packets being sent. Therefore, delay is approximately further doubled. Though this still occurs with end-to-end delays remaining in the tens of millisecond range for the QP's in which video quality is good. This type of delay range is acceptable even for interactive applications but may contribute to additional delay if it forms part of a longer network path.

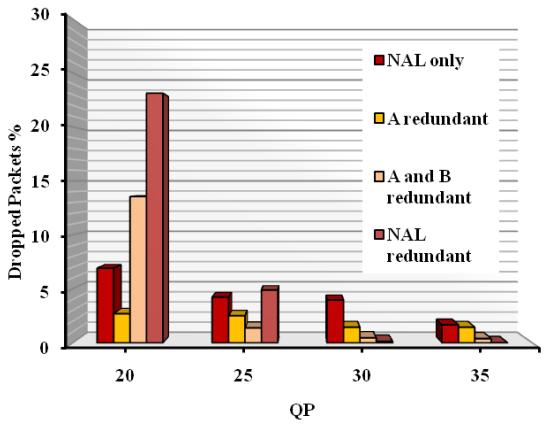

Fig. 2. Dropped packets for protection scheme with 5% intra-refresh MB's for the *Football* sequence ('NAL only' provides no duplicate packets, *A redundant* = duplicate A, *NAL redundant* = A, B, C duplicated).

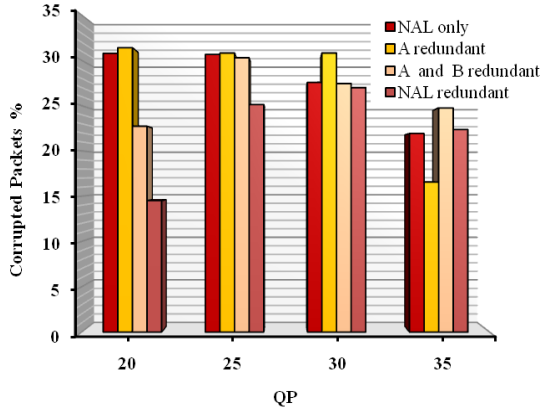

Fig. 3. Corrupted packets for protection scheme with 5% intra-refresh MBs for the Football sequence (*NAL only* provides no duplicate packets, *A redundant* = duplicate A, *NAL redundant* = A, B, C duplicate).

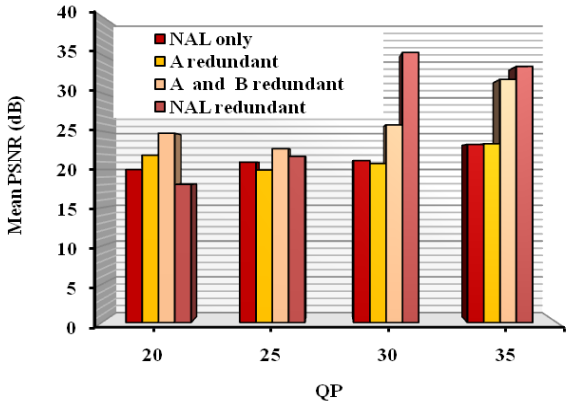

Fig. 4. Video quality (PSNR) for protection scheme with 5% intra-refresh MB's for the Football sequence (*NAL only* provides no duplicate packets, *A redundant* = duplicate A, *NAL redundant* = A, B, C duplicate).

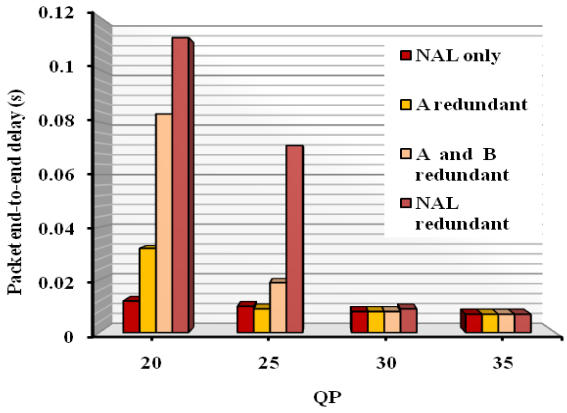

Fig. 5. Packet end-to-end delay for protection scheme with 5% intra-refresh MB's for the *Football* sequence (*NAL only* provides no duplicate packets, *A redundant* = duplicate A, *NAL redundant* = A, B, C duplicate).

Figs. 7-11 present the system performance when redundant NALU's were used to check the effect of a smaller size of the NALU's resulting from applying 2% IR MBs compared to MB line intra update. Better video quality arises with a moderate QP setting and a smaller percentage of IR MB's. Against this must be balanced the difficulty of channel swapping with dispersed IR MBs. On the other hand, by

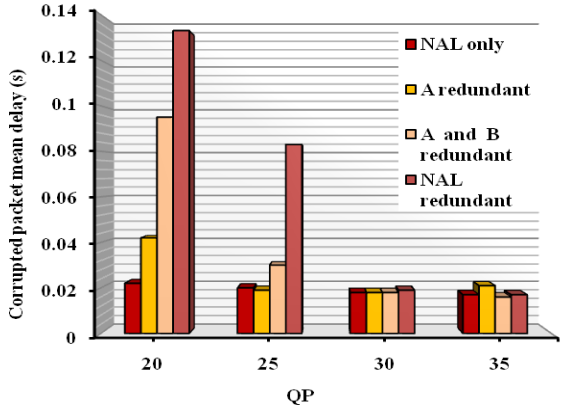

Fig. 6. Corrupted packet end-to-end delay for protection scheme with 5% intra-refresh MBs for the Football sequence (*NAL only* provides no duplicate packets, *A redundant* = duplicate A, *NAL redundant* = A, B, C duplicate).

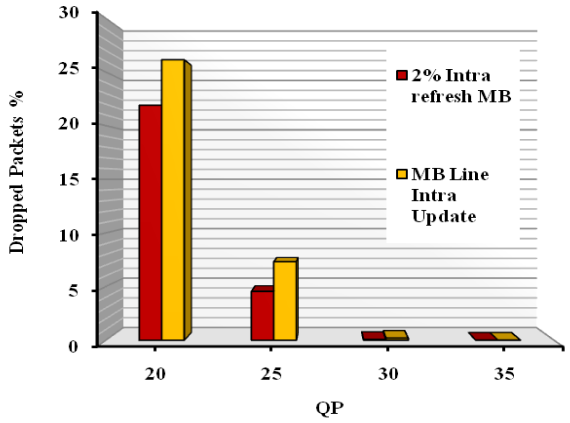

Fig. 7. Dropped packets for either 2% intra-refresh MBs or MB line intra update for *Football*.

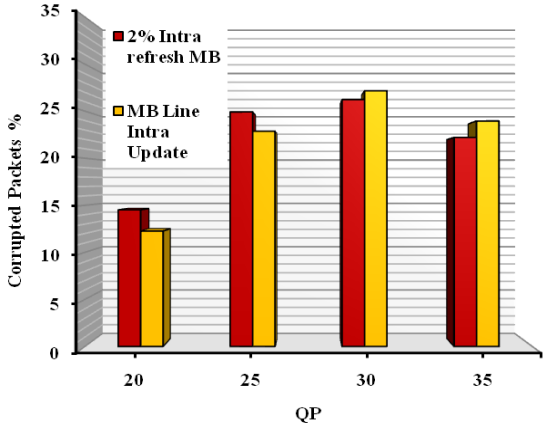

Fig. 8. Corrupted packets for either 2% intra-refresh MBs or MB line intra update for *Football*.

appropriate choice of the IR MB insertion pattern gradual decoder refresh can be achieved [20]. The choice should be governed by the need to maximize the subjective viewing experience during noisy channel conditions.

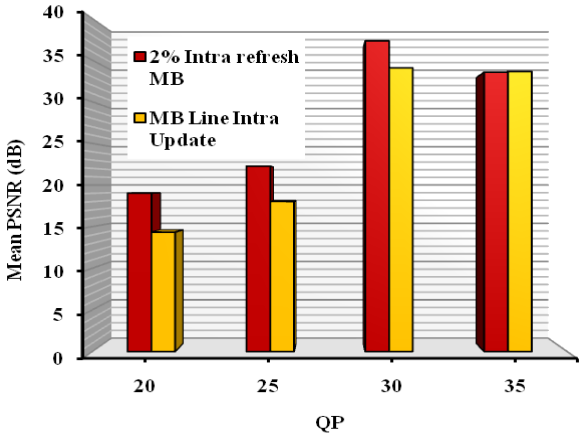

Fig. 9. Video quality (PSNR) for either 2% intra-refresh MBs or MB line intra update for *Football.*

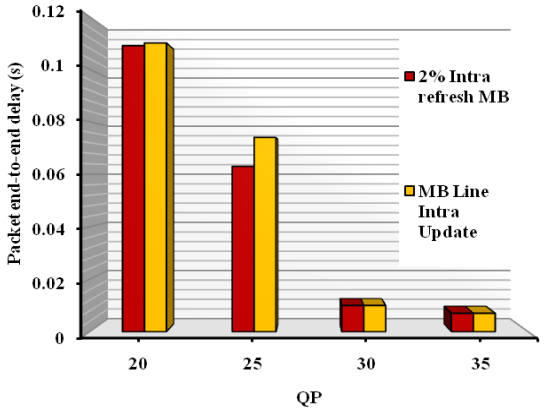

Fig. 10. Packet end-to-end delay for either 2% intra-refresh MBs or MB line intra update for *Football.*

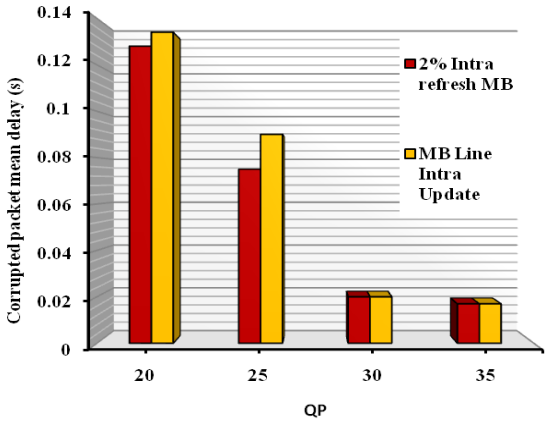

Fig. 11. Corrupted packet end-to-end delay for either 2% intra-refresh MBs or MB line intra update for *Football.*

V. CONCLUSION

Data-partitioning of IPTV video streams is a way of providing graceful quality degradation in a form that will work in both good and difficult wireless channel conditions. This work shows that using Raptor code and duplicate data partitioning with a low percentage of intra-refresh MBs gives a better result in respect to the number of dropped packets and the video quality compared with using MB line intra update. The paper also shows that the choice of a suitable QP (QP=30) will considerably improve the PSNR because of the reduction in packet numbers dropped, which in turn is affected by the size of NALU's. Duplicate partition-A packets at the very least seem essential and probably duplicate partition-B packets will need to also be sent.

REFERENCES

[1] S. Wenger, "H.264/AVC over IP," *IEEE Trans. Circuits Syst. Video Technol.*, vol. 13, no. 7, pp. 645-655, 2003.

[2] T. Wiegand, G.J. Sullivan, G.., Bjontegaard, and A. Luthra, " Overview of the H.264/AVC video coding standard," *IEEE Trans. Circuits Syst. Video Technol.*, vol. 13, no. 7, pp. 560:576, 2003.

[3] A. Shokorallahi, "Raptor codes," *IEEE Trans. Info. Theory*, vol. 52, no. 6, pp. 2551-2567, 2006.

[4] IEEE, 802.16e-2005. "IEEE standard for local and metropolitan Area networks. Part 16: Air interface for fixed and mobile broadband wireless access systems," 2005.

[5] T. Stockhammer, and M. Bystrom, "H.264/AVC data partitioning for mobile video communication," in *IEEE Int'l Conf. Image Proc.*, 2004, pp. 545-548.

[6] J. Radulovic, Y.-K. Wang, S. Wenger, A. Hallapuro, M.H., Hannuksela, and P. Frossard, "Multiple description H.264 video coding with redundant pictures," in *Int'l Workshop on Mobile Video*, 2007, pp. 37-42.

[7] M. Luby, T. Stockhammer, and M. Watson, "Application layer FEC in IPTV services," *IEEE Commun. Mag.*, vol. 46, no. 5, pp. 95-101, 2008.

[8] ETSI TS 102 034 v1.3.1, "Transport of MPEG 2 Transport Stream (TS) Based DVB Services over IP Based Networks," DVB Blue Book A086rev5, http://www.dvb.org/technology/bluebooks, Oct. 2007.

[9] 3GPP TS26.346, "Multimedia Broadcast/Multicast Service (MBMS): Protocols and Codecs," Dec. 2005.

[10] D.J.C. MacKay "Fountain codes," *IEE Proceedings: Commun.*, vol. 152, no. 6, pp. 1062–1068, 2005.

[11] M. Luby "LT codes," in *34rd Ann. IEEE Symp. on Foundations of Computer Science*, 2002, pp. 271–280.

[12] R. Palanki, and J. Yedidai, "Rateless codes on noisy channels." in *Int. Symp. Info. Theory*, 2004, p. 37.

[13] R.M. Schreier, and A. Rothermel, "Motion adaptive intra refresh for low-delay video coding," in *Int'l Conf. on Consumer Electronics*, 2006, pp. 453-454.

[14] Y.J. Liang, K. El-Maleh, and S. Manjunath, "Upfront intra-refresh decision for low-complexity wireless video telephony," In *Int'l Symp. on Circuits and Syst.*, 2006, 4 pages.

[15] M. Luby, T. Gasiba, T. Stockhammer, and M. Watson, "Reliable multimedia download delivery in cellular broadcast networks," *IEEE Trans. Broadcast.*, vol. 53, no. 1, pp. 235-246, 2007.

[16] C. So-In, R. Jain, and A.-K. Tamimi, "Capacity evaluation for IEEE 802.16e mobile WiMAX," *Journal of Computer Systems, Networks, and Commun.* [online], 12 pages, 2010.

[17] G. Haßlinger, and O. Hohlfeld, "The Gilbert-Elliott model for packet loss in real time services on the Internet," in *14th GI/ITG Conf. on Measurement, Modelling, and Evaluation of Computer and Commun. Systs.*, 2008, pp. 269-283.

[18] .J. Liang, J.G. Apostolopoulos, and B. Girod, "Analysis of packet loss for compressed video: Effect of burst losses and correlation between error frames," *IEEE Trans. Circ. Syst. Video Technol.*, vol. 18, no. 7, pp. 861-874, 2008.

[19] F.C.D. Tsai, et al., "The design and implementation of WiMAX module for ns-2 simulator," *Workshop on ns2: the IP network simulator*, 2006, .article no. 5.

[20] M.M. Hannuksela, Y.-K. Wang, and M. Gabbouj, "Random access using isolated areas," in *IEEE Int'l Conf. on Image Process.*, 2003, pp. 841-844.